FEBS 25593 FEBS Letters 510 (2002) 5–9

Hypothesis

F-actin assembly in *Dictyostelium* cell locomotion and shape oscillations propagates as a self-organized reaction–diffusion wave

Michael G. Vicker*

Department of Biology-Chemistry, University of Bremen, Leobener Str./NW2, D-28359 Bremen, Germany

Received 5 September 2001; revised 12 November 2001; accepted 14 November 2001

First published online 27 November 2001

Edited by Amy M. McGough

Abstract The crawling locomotion and shape of eukaryotic cells have been associated with the stochastic molecular dynamics of actin and its protein regulators, chiefly Arp2/3 and Rho family GTPases, in making a cytoskeleton meshwork within cell extensions. However, the cell's actin-dependent oscillatory shape and extension dynamics may also yield insights into locomotory mechanisms. Confocal observations of live *Dictyostelium* cells, expressing a green fluorescent protein–actin fusion protein, demonstrate oscillating supramolecular patterns of filamentous actin throughout the cell, which generate pseudopodia at the cell edge. The distinctively dissipative spatio-temporal behavior of these structures provides strong evidence that reversible actin filament assembly propagates as a self-organized, chemical reaction–diffusion wave.

Key words: Cell locomotion; Oscillation; Self-organization; Autocatalytic wave; Filamentous actin; *Dictyostelium discoideum*

1. Introduction

Actin's primary role in the crawling locomotion of eukaryotic cells has been interpreted in cytoskeleton models focused on stochastic kinetics at the molecular level. Present evidence implicates a large number of proteins as members of a signal cascade, thought to control actin filament (F-actin) dynamics. These proteins include the Scar/WAVE/WASP family [1], which regulates Arp2/3 [2], and some of the small GTPases of the Rho family, e.g. Rac, Rho and Cdc42 [3]. These systems, and other actin-binding proteins [4], including the F-actin-severing protein cofilin [5], have been shown to function as 'on/off' signal switches in the signal cascade or to promote the assembly or interfilament relationships of actin filaments, respectively. Although the important reactions and relationships among these molecules have been identified in considerable detail, little data are available with regard to three main problems concerning cell locomotion: (1) the origin of the adaptive response of cells to a sudden increase in concentration of a stimulant, e.g. a chemoattractant, which rapidly affects the locomotory system [6]; (2) the kinetics and specific operational time-frame of F-actin assembly in relation to that of the Scar/WAVE/Arp2/3 and GTPase systems and the cell surface dynamics they are thought to regulate; (3) studies at the molecular level have not resolved the issue about the origin and significance of oscillations of the eukaryotic cell surface and its protrusions. Thus, the neutrophil surface demonstrates an oscillatory character [7] and fibroblast lamellipodia dynamics are periodic [8].

Cells are vibrating bodies. *Dictyostelium*'s cell surface movements may be quantitatively described and modelled as transient superpositioned wave modes of differing power and frequency [9,10]. Classical, physical standing and travelling wave patterns characterize the cell surface. Analysis of human keratinocytes has produced similar results [11]. Cell locomotion and shape dynamics are thought to reflect the spatio-temporal dynamics of F-actin assembly, which has been visualized in fixed *Dictyostelium* amoebae [12,13] and vertebrate fibroblasts [14] as supramolecular, dissipative F-actin patterns. These patterns demonstrate most of the diagnostic features specifically identifying self-organized chemical wave patterns, as found in purely chemical systems [15,16]. Self-organized, dissipative spatio-temporal patterns have also been reported in tubulin suspensions [17]. Self-organized patterns of F-actin assembly, including double spirals and disks, are clearly evident driving lamellipodia extension in live mouse B16 melanoma cells expressing green fluorescent protein (GFP)–actin [18]. The ubiquity of oscillatory and adaptive cell behavior indicates the possibility that their study may yield significant insights into the evolutionarily deep mechanism of cell locomotion and surface dynamics.

Here I examine F-actin's role in cell shape oscillations and locomotion by means of confocal observations of F-actin behavior in live *Dictyostelium discoideum* amoebae, expressing a GFP–actin fusion protein. The image time and volume series of these cells provide direct, visual evidence of actin's role in these basal cellular processes. The spatio-temporal patterns of GFP–actin strongly support the conclusion that reversible F-actin assembly propagates autocatalytically as a self-organized, chemical reaction–diffusion wave, producing supramolecular F-actin patterns and oscillatory pseudopodial extensions. The results thus complement the present concepts of cell locomotion based exclusively on stochastic molecular kinetics and indicate that self-organized actin waves and nonlinear dynamics are fundamental to eukaryotic cell behavior.

*Fax: (49)-421-218 4042.
E-mail address: vicker@uni-bremen.de (M.G. Vicker).

Abbreviations: GFP, green fluorescent protein; F-actin, filamentous actin

0014-5793/02/$22.00
PII: S0014-5793(01)03207-0

2. Materials and methods

2.1. Cell transformation and culture

D. discoideum strain AX2 was permanently transformed using a novel construct to promote the expression of a GFP–actin fusion protein [19]. Cells were cultured at 21°C in a plastic tissue culture flask in HL5 medium [20] supplemented with 20 μg/ml G418 (Boehringer, Mannheim, Germany). Before confocal observation, cells were washed twice by brief centrifugation in a microcentrifuge and the growth medium was replaced by 17 mM KH_2/K_2HPO_4 buffer, pH 6.5.

2.2. Confocal microscopy and image handling

Images series of live cells expressing GFP–actin were obtained using a Zeiss LSM 410 confocal microscope at 21°C and a 63×1.4 n.a. objective, 10% laser power (excitation 488 nm/emission 510 nm) and a 10 nm pinhole. Each live cell motion time series image was integrated from four confocal snapshots of 0.7 s every 5 s. These conditions reduced bleaching of GFP–actin and cell injury. The objective was focused close to the cell/glass interface. Complete *z*-sections consisted of 30 images 0.2 μm apart. Each image was integrated from only two images of 0.7 s, and are, correspondingly, of lower image quality than the time series images. Densitometric examination employed NIH Image 1.62.

2.3. Cell fixation

Cells were treated with 3.7% formaldehyde in KH_2/K_2HPO_4 buffer and mounted in glycerol/buffer (4:1) as described [12]. Cells were stained with 0.8 μm phalloidin–tetramethylrhodamine-isothiocyanate (TRITC: Sigma, Deisenhof) and photographed using a Leica TCS4D confocal microscope and a 63×1.4 n.a. objective. TRITC was excited at 514 nm and the emission recorded at 543 nm.

3. Results and discussion

Two-dimensional, confocal images of live *Dictyostelium* cells demonstrate striking, closed F-actin bands or disks with diameters ranging from a few micrometers to that of the whole cell, which confocal sectioning reveals as cross-sections though flattened, fully three-dimensional (3-D) spheres or hemispheres (Fig. 1A,B). High-resolution images of similar patterns may also be obtained in fixed cells specifically stained for F-actin (Fig. 1C), indicating their similar origin in GFP–actin-expressing and non-expressing cells. Each F-actin disk or wavefront in Fig. 1C is associated with one pseudopodium in such a way that the anterior half of the disk lies within the pseudopodium and the posterior half within the cell. Each disk center is transected, roughly, by the apparent position of the cell's original boundary, before pseudopodium extension. The morphology of the F-actin disk indicates that F-actin waves propagate internally as well as in the form of pseudopodia, i.e. both posteriorly and anteriorly, and that propagation, and thus F-actin assembly, may be retrograde to and independent of the cell edge. The actin filaments forming such supramolecular patterns may be quite short, because they may become lost if the fixative contains detergent, e.g. Triton X-100 [10]. The F-actin concentration immediately behind the wavefront 'rim' appears greater than that within the cell generally, probably reflecting the concentration of F-actin disassembly products, i.e. oligomers, after wavefront passage.

Selected excerpts from a 15 min locomotion record of one cell (Fig. 2) show that the behavior of F-actin wavefronts appears similar whether they are propagating internally or as a cell extension. Slightly faster propagation at one end of the nominally spherical 3-D wavefront induces it, and the cell, to elongate. Wavefront propagation and radial growth usually continue until wavefront integrity collapses at the point where its curvature and, thus, speed become very low (Fig. 2, 80 s). The propagation speed of chemical wavefronts is directly proportional to wavefront curvature [21]. The complete QuickTime film from which the sequence in Fig. 2 was selected may be downloaded from (http://www1.uni-bremen.de/~vicker).

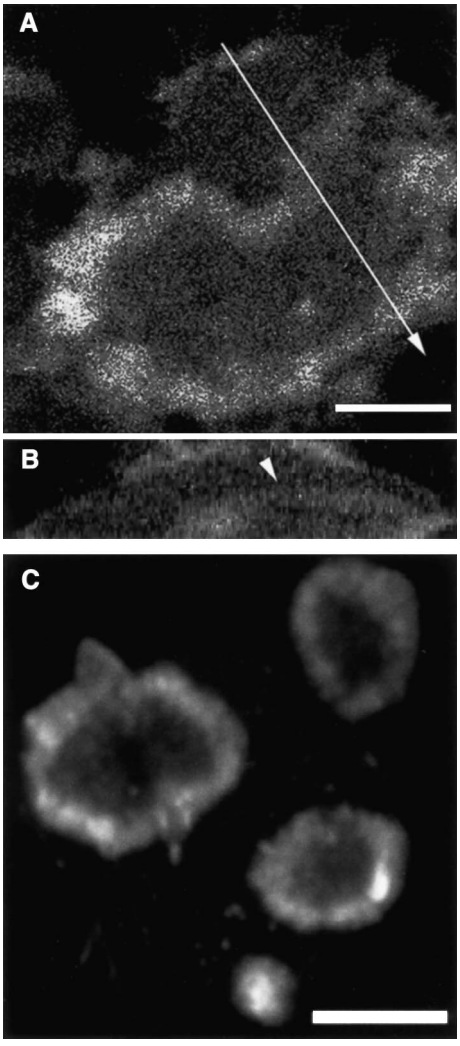

Fig. 1. Confocal images of F-actin autowaves in vegetative-stage *D. discoideum* AX2 cells either live or fixed. A: A live cell expressing a GFP–actin fusion protein [19] demonstrates a large F-actin ring visualized in *xy*-section near the glass substratum. The bar indicates 10 μm. B: A *z*-axis section of the same cell along the path of the arrow in (A) shows the F-actin wavefront to consist of a flattened F-actin sphere or hemisphere (arrowhead). The image measures 20×6 μm. C: A fixed cell stained with phalloidin–TRITC demonstrated four thin disks of F-actin, one apparently nascent, each generating a pseudopodium. The bar indicates 10 μm.

The linearity and diagonal slopes of the space–time plots of the time series image data (Fig. 3) demonstrate that the rate of wavefront advance, here 1.45–2.78 μm/min, is more or less constant and changes little as the intracellular wavefront begins extension as a pseudopodium. Rupture or quenching in other flatter, more labile front sectors either self-repair immediately or induce the development of free wavefront ends. The process of 'repair' appears to generate a locally complex F-actin pattern (Fig. 3A, right side). Such filegrane patterns within F-actin wavefronts at cell boundaries have previously been noted in fixed cells [9,10].

Spherical expansion and disruption at low front curvature

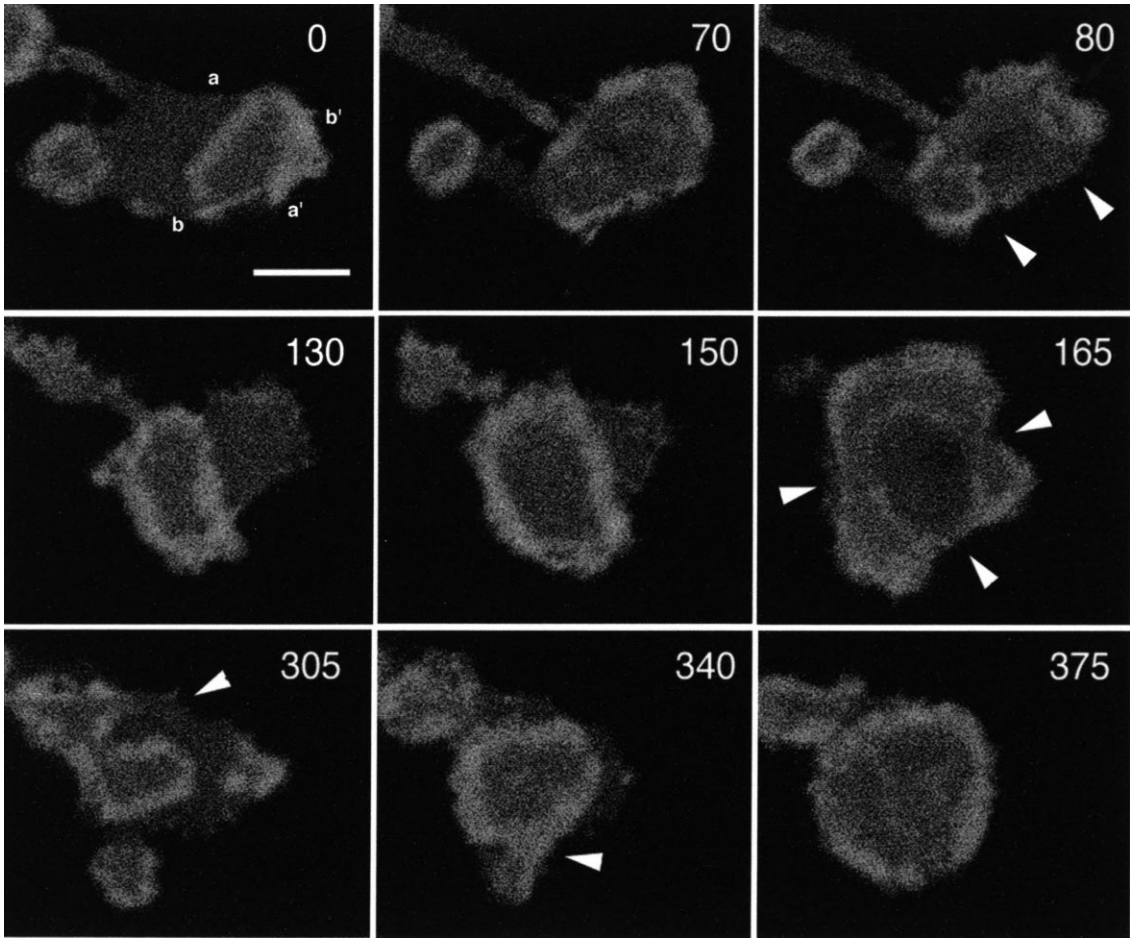

Fig. 2. Selected images from a 15 min time series of one cell locomoting on glass. Cycles of wave expansion and disruption are apparent. Each frame records the time in seconds. Arrowheads indicate points of wavefront collapse and development of 3-D spiral vortex arms (80 s), wavefront collapse (165 s and 305 s), and wavefront expansion and collision with mutual quenching at the point of contact of two wavefronts (340 s). Wavefronts on the right are seen to shrink and vanish as the cell moves to the left (80–150 s and 165–340 s). The letters in frame $t = 0$ s refer to Fig. 3. The bar indicates 10 μm.

are signal features of chemical waves, as are the 3-D spiral vortexes, which develop at the free ends of the 3-D wavefront (looking somewhat like sections through the infolding rims of a mushroom cap) and rapidly propagate into the cell at > 56 μm/min (Fig. 2, 80 s; Fig. 3B). The relationship between the spiral propagation rate and its curvature has been found to be an intrinsic property of self-organized chemical wave systems [15,16]. Thus, the scale of F-actin wavefront spiral curvature relative to the cell's physical dimensions probably determines that locally infolding vortex arms almost invariably collide with other local spirals or other parts of the wavefront. Colliding wavefront spiral ends were seen to anneal, pinch off and form two smaller F-actin spheres, generally polar and orientated normal to their antecedent (Fig. 2, 130, 165 s; Fig. 3B). After vortex elimination through mutual wavefront contact and quenching, the intact F-actin wavefronts reassumed centrifugal expansion. However, some wavefronts produced in this way shrank to extinction, leaving the F-actin-free end of the cell locally motionless. Although shrinkage is an intrinsic feature of chemical wavefronts [15], it is also possible that internal motion of the whole cell might remove all or part of a wavefront from the plane of focus. Colliding wavefronts always mutually extinguished each other at the point of contact (Fig. 2, 340 s), another intrinsic and diagnostic feature specific to dissipative chemical reaction–diffusion wave systems [15,16,21]. Subsequent events of wavefront propagation, elongation, puncture and collapse proceeded cyclically after this pattern. A simple and consistent model of actin wave behavior was made in an attempt to account for and summarize most of the salient, observed features of actin's behavior in the locomotion of vegetative-stage *Dictyostelium* AX2 cells (Fig. 4). F-actin wavefronts in aggregative-stage *Dictyostelium* cells are smaller [19] and, correspondingly, they propagate more rapidly than those seen in the vegetative cell shown here (data not shown).

I have used the generic nature of the spatio-temporal patterns of self-organized wave behavior, as demonstrated in different chemical systems, to help identify the origin of similar patterns of F-actin in *Dictyostelium* cells. Thus, the behavior and morphology of actin waves indicate that these patterns are likely products of instability within a non-equilibrium system. However, further investigation is required of both the role of F-actin waves in the behavioral and molecular processes of eukaryotic cells (especially the role of these waves in pseudopodium induction and advance) and the detailed molecular nature of the propagating wavefront itself. The appearance of large expanding supramolecular 'disks' or spheres of F-actin is inconsistent with previous concepts of locomo-

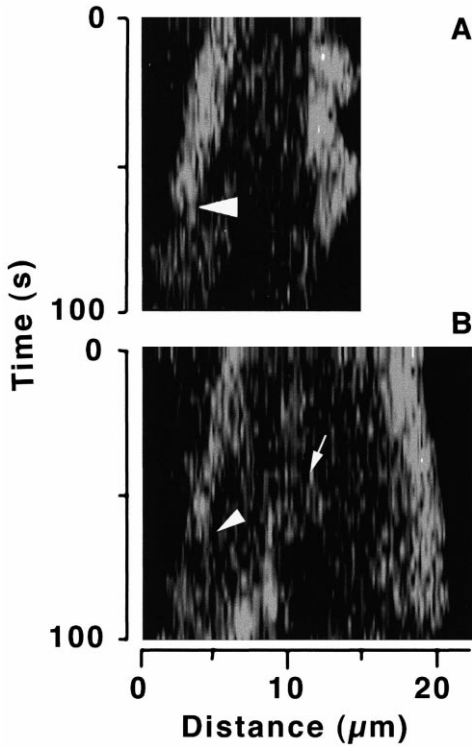

Fig. 3. Two space–time plots of the first 100 s of data from the cell sequence in Fig. 2. A: A densitometric trace starts from point **a** at $t=0$ in Fig. 2 (left in A here) and finishes at point **a′** on the other side of the cell (right in A). The F-actin wavefront at the cell's upper left initially propagates outward (to the left in A), as seen by the slope of the trace and then collapses as its curvature decreases (arrowhead in A). The flat wavefront on the other side of the cell (right in A) undergoes repeated disruption, repair, extension and retraction, but no net outward propagation. The wavefront collapses completely at about 80 s. B: The trace begins from point **b** at $t=0$ in Fig. 2 and finishes at point **b′**. As indicated by the slope of this plot, the wavefront propagates outward at both ends, either within the cell or extending beyond the original cell boundary as a pseudopodium (arrowhead). One F-actin spiral vortex arm appears early in the path of the trace in the middle of the cell at about 40 s (arrow), and becomes increasingly apparent by 80 s.

tory F-actin dynamics based exclusively on stochastic molecular concepts. The spontaneously forming dynamic features reported here, spanning several micrometers and moving rapidly within the cell, do not appear to relate, to my knowledge, to any other known physical object within the cell or to originate as a secondary consequence of yet another, unknown, non-actin carrier process. Pseudopodium formation and F-actin waves may be seen to be directly related in time and space. F-actin's wave behavior indicates an hitherto unidentified physical state of actin and provides support for a novel mechanism accounting for pseudopodium extension and the rotating oscillatory waves, which determine cell surface shape [12,13]. Thus, cell surface dynamics and cell locomotion itself are determined, rather than incoherent or random, processes. F-actin wave propagation also provides support for the idea that self-organization and non-linear kinetics are universal, intrinsic and fundamental principles of eukaryotic cells, with possible consequences for concepts of cellular time and the origin of some biological oscillations, and for multicellular system development.

The F-actin wavefront propagates with undiminished rim density despite its considerable radial expansion, i.e. there seems to be little or no thinning out of the rim until its dissolution. This apparent time-dependent increase in filament number and, thus, filament nucleation within the wavefront might indicate that a filament-severing protein such as cofilin [5,22] is necessary to fission F-actin and thus amplify the number of filaments and growth-competent filament ends to foster wave advance. A role for other proteins in wave propagation remains even less realistic. One may speculate that the complexity inherent in the Scar/Arp2/3 and GTPase signal cascade systems might itself offer ample scope for the development of non-linear system behavior. Thus, adaptation and time delays, which characterize non-linear systems, also appear along the chain of molecular reactions leading to F-actin assembly and might be expected to induce self-organization in the regulation of actin assembly. The relationship of these reactions to that of F-actin assembly and disassembly itself within the wavefront is, however, entirely unknown. Thus, several of the chief regulatory proteins of F-actin assembly, e.g. Scar/WAVE [1], Arp2/3 [23], DGAP [24] and A6/Twinfilin [25], have been visualized concentrated at the leading edge of

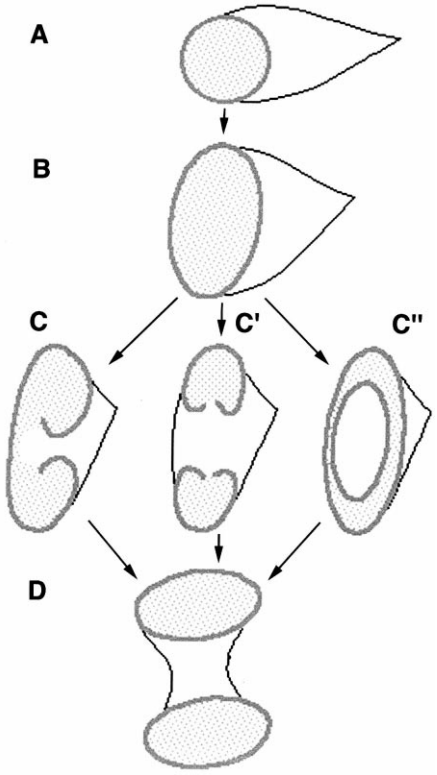

Fig. 4. A model of cyclical F-actin wavefront dynamics. A, B: The polar, radial expansion of an *xy*-section of a 3-D F-actin wavefront (heavy line). The shading is meant to represent the disassembly products of F-actin appearing behind the wavefront. C: Three alternative views of the disruption of the 3-D wavefront, which occurs at low front curvature. Live cells usually show one of the three figures sketched here. A wavefront break may occur either laterally (one or both sides: C or C′, respectively) or C″ – dorsally or ventrally (producing a similar picture). Following local collapse of the wavefront, spiral vortex arms develop swiftly at all free edges. Visualization of the development of this event is complicated by its 3-D nature. D: The spiral arms of the surviving daughter wavefront(s) anneal with parts of the wavefront (and thus disappear) as the wavefronts consolidate before initiating radial propagation, which tends to be oriented normal to the original wavefront (B).

active lamellipodia: a fact thought to implicate their function. However, no such concentration of these proteins appears associated with the propagating F-actin wavefront during its transit elsewhere through the cell. Therefore, consideration should be given to the possibility that although much current evidence supports a role for these regulatory proteins at the edge of lamellipodia or pseudopodia, a role for them in F-actin wave propagation and in the F-actin wave-driven process of extension itself has yet to be demonstrated. The relative timing of the appearance of these regulatory proteins vs. F-actin waves at developing lamellipodia/pseudopodia ought to be subjected to investigation. The apparently autocatalytic nature of the wavefront, the self-organized features of its propagation and the global properties of its spatial and temporal generation within the cell are possible evidence for significant differences between the regulation and existence of wavefront F-actin and that in the cytoskeleton.

Acknowledgements: *D. discoideum* strain AX-2 cells, expressing a novel GFP–actin fusion protein, were generously supplied by G. Gerish (Martinsried, Germany).

References

[1] Hahne, P., Sechi, A., Benesch, S. and Small, J.V. (2001) FEBS Lett. 492, 215–220.
[2] Bailly, M., Ichetovkin, I., Grant, W., Zebda, N., Machesky, L.M., Segall, J.E. and Condeelis, J. (2001) Curr. Biol. 11, 620–625.
[3] Tapon, N. and Hall, A. (1997) Curr. Opin. Cell Biol. 9, 86–92.
[4] Noegel, A.A. and Luna, J.E. (1995) Experientia 51, 1135–1143.
[5] Southwick, F.S. (2000) Proc. Natl. Acad. Sci. USA 97, 6936–6938.
[6] Vicker, M.G. (1994) J. Cell Sci. 107, 659–667.
[7] de Bruyn, P.P.H. (1946) Anat. Rec. 95, 177–192.
[8] Abercrombie, M., Heaysman, J.E.M. and Pegrum, S.M. (1970) Exp. Cell Res. 59, 393–398.
[9] Vicker, M.G., Xiang, W., Plath, P.J. and Wosniok, W. (1997) Physica D 101, 317–332.
[10] Vicker, M.G. (2000) Biophys. Chem. 84, 87–98.
[11] Alt, W., Brosteanu, O. and Hinz, B. (1995) Biochem. Cell Biol. 111, 2513–2526.
[12] Killich, T., Plath, P.J., Xiang, W., Bultmann, H., Rensing, L. and Vicker, M.G. (1993) J. Cell Sci. 106, 659–667.
[13] Killich, T., Plath, P.J., Haß, E.-C., Xiang, W., Bultmann, H., Rensing, L. and Vicker, M.G. (1994) BioSystems 33, 75–87.
[14] Blume-Jensen, P., Claesson-Welsh, L., Siegbahn, A., Zsebo, K.M., Westermark, B. and Heldin, C.-H. (1991) EMBO J. 10, 4121–4128.
[15] Winfree, A.T. and Strogatz, S.H. (1984) Nature (Lond.) 311, 611–615.
[16] Scott, S.K. and Showalter, K. (1992) J. Phys. Chem. 96, 8702–8711.
[17] Mandelkow, E., Mandelkow, E.-A., Hotani, H., Hess, B. and Müller, S.C. (1989) Science 246, 1291–1293.
[18] Ballestrem, C., Wehrle-Haller, B. and Imhof, B.A. (1998) J. Cell Sci. 111, 1649–1658.
[19] Westphal, M., Jungbluth, A., Heidecker, M., Mühlbauer, B., Heizer, C., Schwartz, J.-M., Marriott, G. and Gerisch, G. (1997) Curr. Biol. 7, 176–183.
[20] Sussman, M.M. (1987) Methods Cell Biol. 28, 9–29.
[21] Jahnke, W., Henze, C. and Winfree, A.T. (1988) Nature (Lond.) 336, 662–665.
[22] Lappalainen, P. and Drubin, D.G. (1997) Nature (Lond.) 388, 78–82.
[23] Svitkina, T.M. and Borisy, G.G. (1999) J. Cell Biol. 145, 1009–1026.
[24] Faix, J., Clougherty, C., Konzok, A., Mintert, U., Murphy, J., Albrecht, R., Mühlbauer, B. and Kuhlmann, J. (1998) J. Cell Sci. 111, 3059–3071.
[25] Vartiainen, M., Ojala, P.J., Auvinen, P., Peränen, J. and Lappalainen, P. (2000) Mol. Cell. Biol. 20, 1771–1783.